

Searching for the high-energy neutrino counterpart signals: The case of the Fermi bubbles signal and of dark matter annihilation in the inner Galaxy

Ilias Cholis^{1,2,*}¹*SISSA, Via Bonomea, 265, 34136 Trieste, Italy*²*INFN, Sezione di Trieste, Via Bonomea 265, 34136 Trieste, Italy*

(Received 10 June 2012; published 23 September 2013)

The recent uncovering of the Fermi bubbles/haze in the Fermi γ -ray data has generated theoretical work to explain such a signal of hard γ rays in combination with the WMAP haze signal. Many of these theoretical models can have distinctively different implications with regards to the production of high-energy neutrinos. We discuss the neutrino signals from different models proposed for the explanation of the Fermi bubbles/haze, more explicitly, from dark matter annihilation in the galactic halo with conditions of preferential cosmic ray diffusion, from recent active galactic nucleus jet activity, from periodic diffusive shock acceleration, from stochastic second order Fermi acceleration and from long time-scale star formation in the galactic center in combination with strong galactic winds. We find that some of these models will be probed by the IceCube DeepCore detector. Moreover, with a km^3 telescope located in the Northern Hemisphere, we will be able to discriminate between the hadronic, leptonic and the dark matter models. Additionally using the reconstructed neutrino spectra we will probe annihilation of TeV scale dark matter towards the galactic center.

DOI: [10.1103/PhysRevD.88.063524](https://doi.org/10.1103/PhysRevD.88.063524)

PACS numbers: 95.35.+d

I. INTRODUCTION

Using the first year of Fermi LAT γ -ray full sky data, the authors of [1] revealed the presence of a diffuse component towards the galactic center that extends up to 50° in latitude. That component has a spectrum significantly harder than elsewhere in the Galaxy [1–3] and a morphology elongated in latitude to longitude that, depending on the exact template analysis used for its extraction from the full sky data, is either well defined within two bubbles with distinct edges both at high and low latitudes [2], known as the “Fermi bubbles,” or is slightly more diffuse (the “Fermi haze”) with a latitude to longitude axis ratio of ≈ 2 [3] but still confined within $|l| \lesssim 20^\circ$ and $|b| \lesssim 50^\circ$ and with the “edges” seen only at the higher latitudes [3].

The signal of hard γ rays together with the WMAP haze [4,5] may indicate the presence of a hard component of cosmic ray (CR) electrons, which through their up-scattering of low-energy photons produce the hard spectrum of (inverse Compton) γ rays and through their synchrotron radiation the hard observed spectrum at microwaves. Various authors have suggested mechanisms for the origin of these CR electrons. Among them, possible scenarios include recent (1–3 Myr ago) AGN jet activity in the galactic center [6,7]; TeV scale dark matter (DM) annihilating to leptons [3,8], within conditions of preferential diffusion perpendicular to the plane [3]; stochastic second order Fermi acceleration by large scale turbulence in magneto-sonic waves [9]; or periodic injection of hot plasma causing diffusive shock acceleration (first order Fermi acceleration) in the halo [10].

Alternatively, CR protons associated with long time-scale (\sim Gyr) star formation in the galactic center, transferred by strong winds into the Fermi bubbles region, have been suggested by [11]. Finally, a combination of DM and millisecond pulsars in the galactic halo adding up to the signals at γ rays and microwaves has been discussed in [12].

The detection or lack of high-energy neutrinos from km^3 neutrino telescopes could help discriminate between the leptonic [3,6,7,9,10] and the hadronic [11] scenarios, since the leptonic scenarios would not produce any neutrinos, or a few and up to the TeV scale, while the hadronic explanation of [11] would produce abundant neutrinos up to the PeV scale [13,14] (see also the discussion in [15]).

In addition to discriminating among different models for the Fermi haze/bubbles via searching for their neutrino counterpart, such searches can be used as another channel of indirect DM searches.

DM composes approximately 85% of the matter density of the Universe, yet its particle physics properties still remain unknown. Measurements of CRs [16–22] have generated new model building [8,23–34] and have helped place new constraints on dark matter properties [35–39]. Since many of these models and constraints are placed at the TeV mass scale and suggest or refer to enhanced (boosted) annihilation cross sections with hard spectra for the Standard Model (SM) particle annihilation products, neutrino signals from the galactic center (GC) [40] from the Sun [41] or the Earth [42] can be considered of interest.

IceCube at the South Pole [43,44] has already presented some early (pre-DeepCore) results [45–47] and is expected, with its DeepCore update, to better probe the region that is sensitive for DM searches and has $\lesssim 100$ GeV in neutrino energy. ANTARES, located in

*ilias.cholis@sissa.it

the Mediterranean, is also collecting data [48–50] and, because of its location, probes the GC significantly better than IceCube but, because of its small size, still has a low number of statistics. Finally a future km³ telescope located in the Mediterranean as KM3NeT [51–53] will combine the virtues of IceCube and ANTARES, providing a good neutrino telescope for searches of DM annihilation towards the GC.

In Sec. II we will discuss the neutrino signals of various DM models that could explain the Fermi haze and WMAP haze signals as presented in [3], for both IceCube and a future km³ telescope located in the Northern Hemisphere (using the Mediterranean as the Earth’s latitude of reference), also presenting search strategies for those signals. We use simulated performance information published for the KM3NeT [51,52]. We will extend in Sec. III the discussion of searching for signals in neutrinos towards the GC from more generic DM models. In Sec. IV we will describe the neutrino predictions of the hadronic model of [11] for the Fermi bubbles that, if true, should soon be seen. In Sec. V we discuss why we do not expect any significant signal in neutrinos from the non-DM leptonic models of [6,7,9,10] presented for the bubbles, and we conclude in Sec. VI.

In this work we will discuss the upward going ν_μ flux expected to be measured at the ongoing and future telescopes. For a comparison of the upward going muon events’ rate and the rate of fully contained muons produced by neutrinos inside the detector, see the discussion in [54].

II. EXCITING DARK MATTER ANNIHILATION, CONNECTING TO THE FERMI HAZE AND THE WMAP HAZE

In the context of DM annihilating to leptons, the authors of [3] invoked preferential (anisotropic) diffusion of CR electrons perpendicular to the galactic disk due to ordered magnetic fields in the same direction. Such conditions could explain the Fermi haze spectrum and morphology in combination with the WMAP haze spectrum and angular profile (see Figs. 7 and 8 of [3]).

In that case, exciting dark matter (XDM) [55] was considered, where DM particles with mass $m_\chi = 1.2$ TeV annihilate into a pair of scalar bosons ϕ that then decay to a pair of e^\pm due to kinematic suppression for the case of $m_\phi < 2m_\mu$. In such a case, the energy released by the DM annihilation goes to e^\pm , which have a hard enough spectrum to explain the haze signals [3,8].

Also in an XDM scenario, as has been shown in [23], the annihilation cross section can be enhanced up to $O(10^3)$ to motivate the necessary boost factor (BF) on the annihilation rates that have been invoked to explain the CR positron fraction and $e^- + e^+$ flux excesses [24,56,57]. Thus the magnitude of the annihilation rate needed to explain the Fermi and WMAP haze signals (BF ≈ 30) is naturally

explained within the context of an XDM annihilating to final state SM leptons. Finally, since from cold dark matter (CDM) cosmological simulations [58–60] the DM halo profiles are typically triaxial, a prolate DM profile has been used in [3], with its axis perpendicular to the galactic disk. Observations of the spatial distribution of Milky Way satellites suggest a prolated DM halo with its major axis perpendicular to the stellar disk [61], in agreement with suggestions by hydrodynamic simulations of galaxies with stellar disks [62].

For the case when the SM leptons from the ϕ decay are e^\pm ($m_\phi < 2m_\mu$), no neutrinos are produced; thus the presence of a possible “neutrino haze” is excluded. Alternatively, for $m_\phi > 2m_\mu$ the decay to μ^\pm is allowed and a neutrino haze can exist. To maximize the possible neutrino haze signal and also to explain the Fermi and WMAP signals, we will consider the case where $m_\chi = 2.5$ TeV particles annihilate to a pair of ϕ ’s that decay with a BR = 1 to μ^\pm [63]. The mass of 2.5 TeV is chosen to produce (after the muons decay) e^\pm which during propagation will give similar synchrotron and IC signals. The necessary enhancement in the annihilation rate is BF ≈ 150 to produce the same total injected energy in high-energy e^\pm (see, for instance, Figs. 6 and 7 of [56]).

Since neutrinos do not diffuse or lose energy, the neutrino signal from the DM halo will be identical to the annihilation rate profile $\sim \int \langle \sigma v \rangle \rho_{\text{DM}}^2 dl d\Omega$, with l being the line of sight, $d\Omega$ the angle of observation, ρ_{DM} the DM density and $\langle \sigma v \rangle$ the velocity averaged annihilation cross section (more accurately written as $\langle \sigma | v | \rangle$). Since in the Sommerfeld enhancement case, the $\langle \sigma v \rangle$ depends on the velocity dispersion [23,64–66], it may also have a profile within the main halo (see, for instance, [67]). This does not include effects of substructure, which may make the position dependence of the averaged (after integration) annihilation cross section $\langle \sigma v \rangle$ over the Galaxy even more evident [68].

In Fig. 1 we show the case of 3×10^4 neutrino simulated events for a prolate DM Einasto profile described by

$$\rho(z, R) = \rho_0 \exp\left[\frac{2}{\alpha} \frac{R_0^\alpha}{R_c^\alpha}\right] \exp\left[-\frac{2}{\alpha} \left(\frac{R^2}{R_c^2} + \frac{z^2}{Z_c^2}\right)^{\alpha/2}\right] \quad (1)$$

with $\rho_0 = 0.4$ GeV cm⁻³ the local DM density [69,70], $\alpha = 0.17$, $Z_c/R_c = 2$ and $Z_c = 27$ kpc (giving as much of a total amount of DM mass within the inner 100 kpc as does the spherically symmetric case of $Z_c = R_c = 25$ kpc) [71].

The cases of a homogeneous $\langle \sigma v \rangle$ in Fig. 1 (left) and of $\langle \sigma v \rangle \propto r^{1/4}$ in Fig. 1 (right) (with r the galactocentric distance) are shown. The latter dependence can be the case for the Sommerfeld models [8], as cosmological simulations with DM and baryons have suggested a profile of increasing velocity dispersion towards the GC (compared to the local values) and up to the inner 1 kpc [72–75]. The profile with the $\propto r^{1/4}$ cross section is slightly more

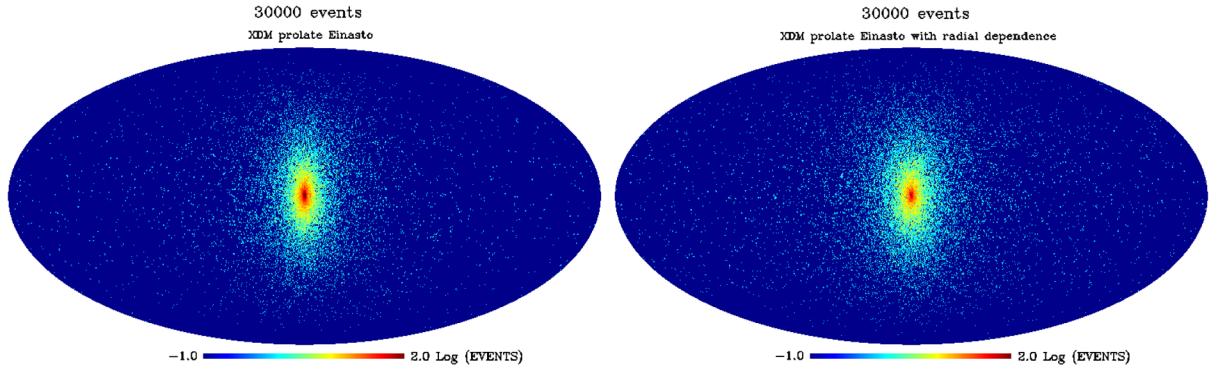


FIG. 1 (color online). 3×10^4 simulated ν events, from the XDM to μ^\pm scenario. Left: Prolate Einasto profile with homogeneous enhancement. Right: Including a $\propto r^{1/4}$ in the annihilation cross section. The latter case is less prolate in its morphology. We present the neutrino maps in Mollweide projection using HEALPix [134].

diffused and less elongated. Since the exact DM profile in the inner 5° of the galactic center is very uncertain, we will derive our conclusions ignoring that part of the DM halo. Additionally, TeV neutrino sources either point or diffuse (from inelastic collisions of CR nuclei with dense ISM gas) are concentrated along the galactic disk. The thin galactic disk, where continuous star formation takes place, has a characteristic (for exponentially decreasing) scale height of 0.3 kpc [76]. This scale height is indicative of the majority of the TeV neutrino sources [77]. The HI interstellar medium (ISM) gas also has a scale height that, towards the GC, is ≈ 0.15 kpc and increases up to 0.3 kpc at the solar ring [79,80], while the H2 gas has a scale height of 0.1 kpc [81,82]. These scale heights are indicative of the galactic diffuse TeV neutrino flux [83] (see also [85]). Thus we will avoid the entire inner 5° in $|b|$.

The neutrino flux at the Earth due to DM annihilation from an angle $d\Omega$ ignoring oscillation ($\phi_{\nu_i}^0$) is described by [86]

$$\frac{d\phi_{\nu_i}^0}{dE_{\nu_i}} = \int d\Omega \int_{\text{l.o.s.}} d\ell(\theta) \frac{\rho_{\text{DM}}^2 \langle \sigma v \rangle(\ell, \theta)}{8\pi m_\chi^2} \frac{dN_{\nu_i}}{dE_{\nu_i}}, \quad (2)$$

where we have left $\langle \sigma v \rangle(\ell, \theta)$ to depend on the position in the Galaxy for the most generic case. A boost factor is absorbed in ρ_{DM}^2 and/or $\langle \sigma v \rangle$. The $\frac{dN_{\nu_i}}{dE_{\nu_i}}$ is the neutrino spectrum of the species ν_i . The multiplicity M^i of the ν_i 's per annihilation event is absorbed in $\frac{dN_{\nu_i}}{dE_{\nu_i}}$, giving

$$\int_0^{m_\chi} \frac{dN_{\nu_i}}{dE_{\nu_i}} dE = M^i. \quad (3)$$

In this work we discuss only the upward going ν_μ flux. The A_{eff} of ν_e upward for both the IceCube DeepCore (not optimally placed for the GC searches) [44] and the KM3NeT [87] is smaller for ν_e 's by at least a factor of 2 at all energies of interest. For simplicity we are going to ignore their contribution.

The observed ν_μ flux at the Earth after oscillations is given by [47,88,89]

$$\phi_{\nu_\mu} \approx \frac{1}{2}(\phi_{\nu_\mu}^0 + \phi_{\nu_\tau}^0) + \frac{1}{8}s_2 \quad \text{with} \\ s_2 = \sin^2 2\Theta_{12}(2\phi_{\nu_e}^0 - \phi_{\nu_\mu}^0 - \phi_{\nu_\tau}^0) \quad \text{and} \quad (4)$$

$$\sin^2 2\Theta_{12} = 0.86,$$

where $\phi_{\nu_i}^0$ is the flux at injection of flavor species ν_i .

For specific experiments one has to include the strong dependence of the telescope's effective area with angle and energy. Within an angle $d\Omega$ and an energy range $E-E+\Delta E$, the total number of upward going $\nu_\mu + \bar{\nu}_\mu$ events is [90]

$$N_{\nu_\mu, \bar{\nu}_\mu}(E, d\Omega) = \int_{E'}^{E'+\Delta E'} dE' \int d\Omega \int_{\text{l.o.s.}} d\ell(\theta) \frac{\rho_{\text{DM}}^2 \langle \sigma v \rangle}{8\pi m_\chi^2} \\ \times A_{\text{eff}, \nu_\mu, \bar{\nu}_\mu}(E', \theta) \frac{dN_{\nu_\mu, \bar{\nu}_\mu}^{\text{osc}}}{dE'_{\nu_\mu, \bar{\nu}_\mu}}, \quad (5)$$

where

$$\frac{dN_{\nu_\mu, \bar{\nu}_\mu}^{\text{osc}}}{dE'_{\nu_\mu, \bar{\nu}_\mu}} = \frac{1}{2} \left(\frac{dN_{\nu_\mu, \bar{\nu}_\mu}}{dE'_{\nu_\mu, \bar{\nu}_\mu}} + \frac{dN_{\nu_\tau, \bar{\nu}_\tau}}{dE'_{\nu_\tau, \bar{\nu}_\tau}} \right) \\ + \frac{1}{8} 0.86 \left(2 \frac{dN_{\nu_e, \bar{\nu}_e}}{dE'_{\nu_e, \bar{\nu}_e}} - \frac{dN_{\nu_\mu, \bar{\nu}_\mu}}{dE'_{\nu_\mu, \bar{\nu}_\mu}} - \frac{dN_{\nu_\tau, \bar{\nu}_\tau}}{dE'_{\nu_\tau, \bar{\nu}_\tau}} \right) \quad (6)$$

For the $\frac{dN_{\nu_i}}{dE_{\nu_i}}$ originating from the 2.5 TeV XDM to muon case, the injection spectra of $\nu_\mu, \bar{\nu}_\mu, \nu_e, \bar{\nu}_e$ (there are no ν_τ 's) are practically identical to those of the injected e^\pm given in Appendix A of [92]. Per annihilation event there are two neutrinos (and two antineutrinos) for each flavor.

Having excluded the $|b| < 5^\circ$ region, the basic remaining background is that of the atmospheric upward neutrinos. The atmospheric background flux is isotropic after averaging for the many different directions of the neutrino telescope's axis within long time scales. For the atmospheric ν_μ and $\bar{\nu}_\mu$ spectra and fluxes above 10 GeV and up to 10 TeV, we used the tables of Appendix B of [93],

extrapolating to higher energies with a spectral power law of 3.7 for the differential spectrum [40].

In Fig. 2 we give in galactic coordinates 10 year mock maps for $\nu_\mu + \bar{\nu}_\mu$ upward events with energy between 360 and 2160 GeV. The energy range has been chosen to optimize the detection of a DM signal for the specific 2.5 TeV XDM case.

The atmospheric background $\nu_\mu + \bar{\nu}_\mu$ events that are shown in the top left of Fig. 2 are 152784, while the DM

events for the prolate Einasto are 424 and 332 for the case of $\langle\sigma v\rangle \propto r^{1/4}$ for the entire sky. Those numbers of DM events are smaller than the 1σ deviation (for the entire sky). Since the morphology of the DM signal is much different than that of the atmospheric background, one can expect to see a signal increase of events towards the GC (see the bottom row of Fig. 2, where we show the inner $60^\circ \times 60^\circ$). Including the $|b| < 5^\circ$ mask for the TeV sources (point and diffuse) for the galactic center and

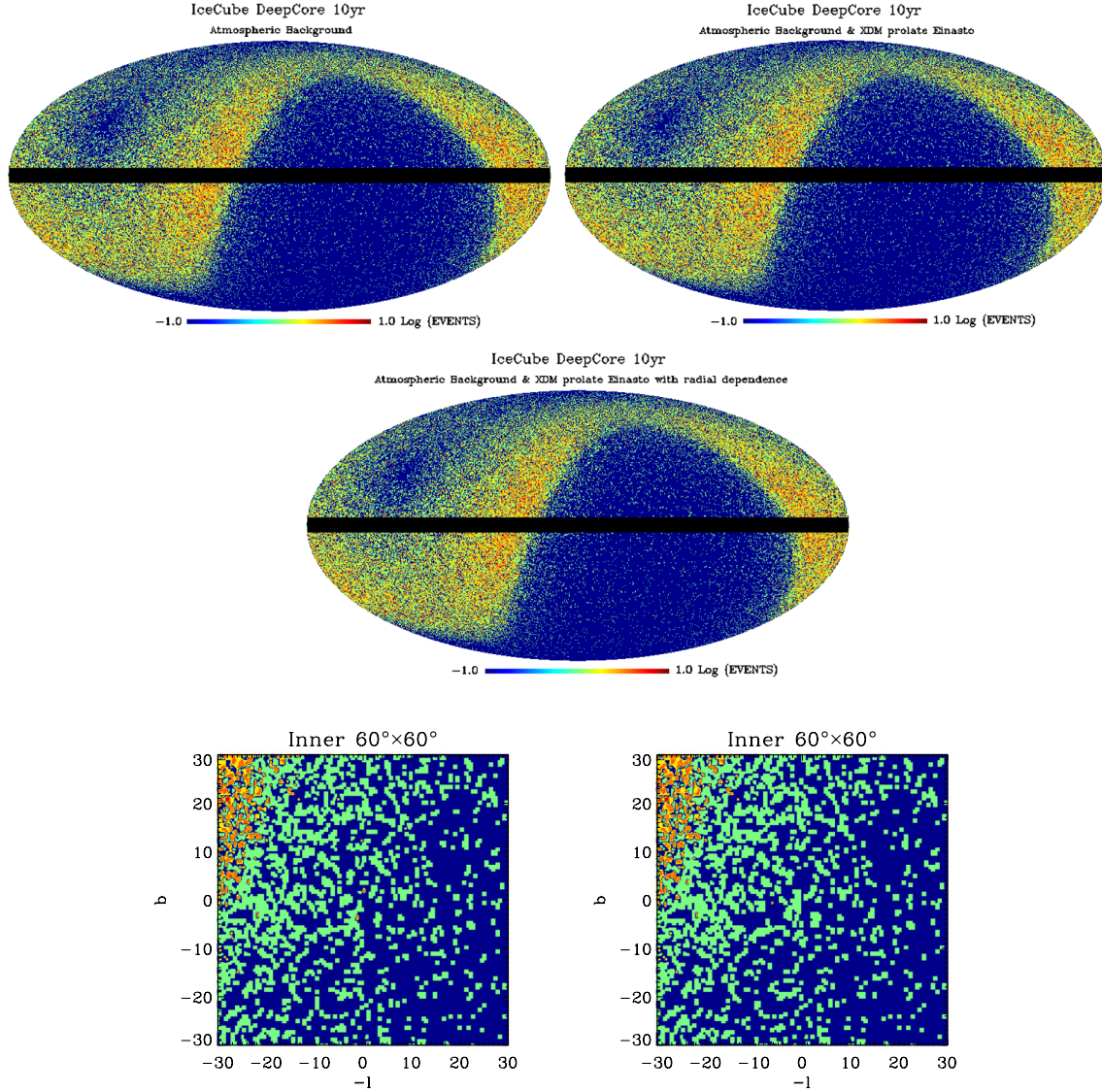


FIG. 2 (color online). IceCube DeepCore $\nu_\mu + \bar{\nu}_\mu$ events after 10 years of data collected with an “online filter” [44] with energy between 360 and 2160 GeV. For the calculations we use the angular dependence for A_{eff} of [43]. Top left: Just atmospheric background, 152784 $\nu_\mu + \bar{\nu}_\mu$ events. Top right: Atmospheric background (152784 $\nu_\mu + \bar{\nu}_\mu$ events) and DM annihilation contribution (424 $\nu_\mu + \bar{\nu}_\mu$ events) from the prolate Einasto profile with homogeneous annihilation cross-section enhancement. Middle: Atmospheric background (152784 $\nu_\mu + \bar{\nu}_\mu$ events) and DM annihilation contribution (332 $\nu_\mu + \bar{\nu}_\mu$ events) from the prolate Einasto profile with $\propto r^{1/4}$ annihilation cross-section enhancement. Numbers refer to the entire sky. We mask out the $|b| < 5^\circ$ to account for neutrinos from point sources concentrated on the disk and from galactic diffuse emission also concentrated on the disk (see text for more details). Bottom left: Inner $60^\circ \times 60^\circ$ for the atmospheric and the XDM prolate profile case. Bottom right: Same region as in bottom left for the case of atmospheric background and XDM prolate Einasto with radial dependence. The neutrinos from the GC are minimally enhanced.

disk, most of this dim DM contribution is hidden. In fact since for IceCube the neutrino events are minimally enhanced in the GC and TeV neutrino point sources and the diffuse galactic neutrinos are also expected to contribute in that region of the sky, a claim for DM cannot be made. Thus for the IceCube DeepCore the sensitivity towards the GC is still too low and the angular resolution (not accounted for here) too large ($\geq 5^\circ$) to provide a robust signal for that DM model.

For a km^3 telescope in the Northern Hemisphere the situation can be very different. In Fig. 3 we give the

expected 3 year mock maps of reconstructed events using the HOURS simulation [51] for KM3NeT [94]. In that case, by comparing Fig. 3 top left, where we show only the atmospheric background simulated events, with Fig. 3 top right (for combined DM Einasto prolate and the atmospheric background), and middle (for the prolate Einasto with $\langle\sigma v\rangle \propto r^{1/4}$ plus atmospheric), one can see a clear indication of a signal from the 2.5 TeV XDM to muons model used to explain the combination of Fermi and WMAP haze signals. Concentrating on the inner $60^\circ \times 60^\circ$ window for the case of a simple Einasto profile, the signal

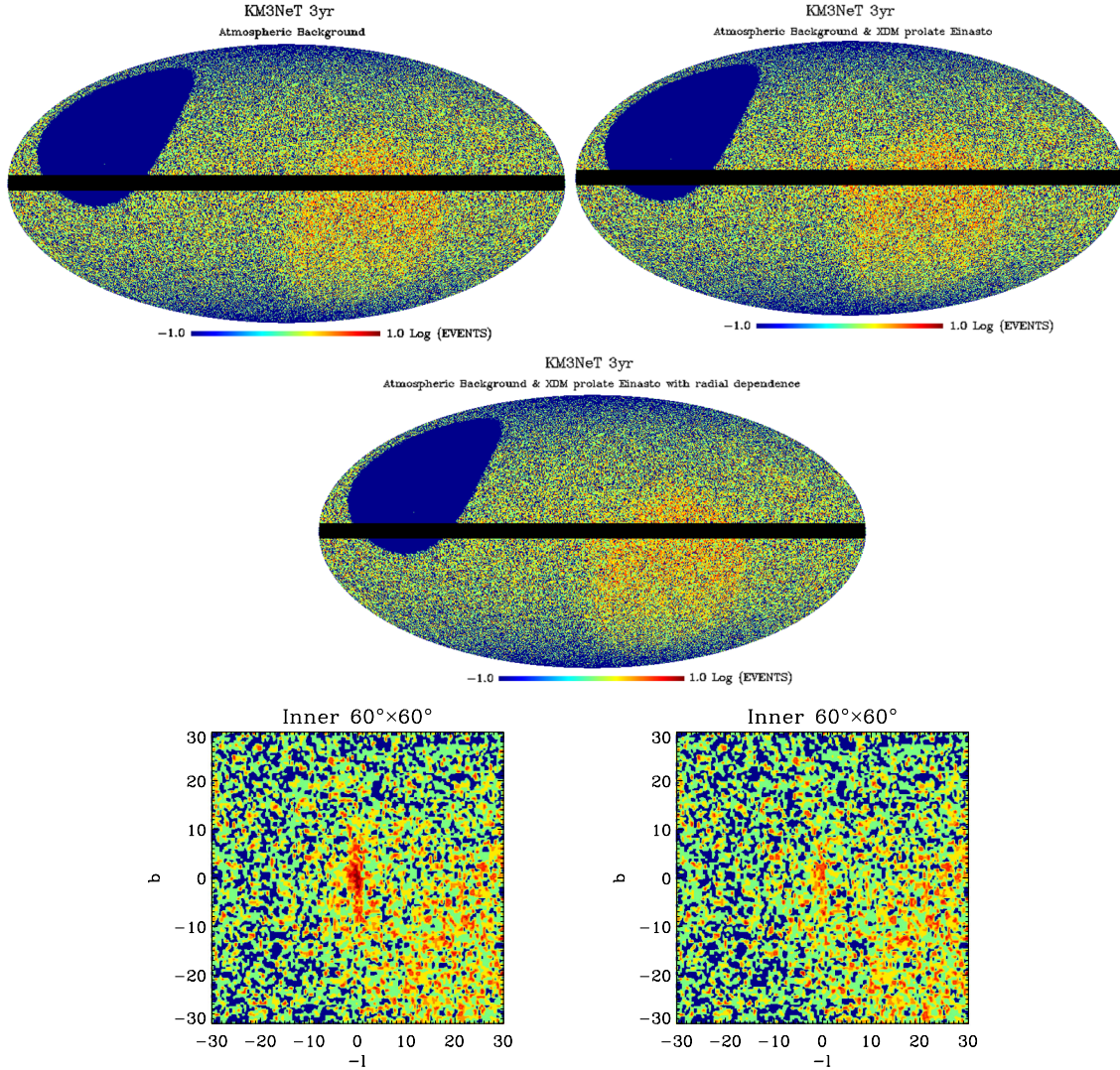


FIG. 3 (color online). KM3NeT $\nu_\mu + \bar{\nu}_\mu$ events after 3 years of data reconstructed by the HOURS [51] package with energy in the range of 360–2160 GeV. We use for KM3NeT the same angular dependence of A_{eff} as for ANTARES [50] due to their expected similar geographic latitude location. Top left: Just atmospheric background, 212446 $\nu_\mu + \bar{\nu}_\mu$ events. Top right: Atmospheric background (212446 $\nu_\mu + \bar{\nu}_\mu$ events) and DM annihilation contribution (2412 $\nu_\mu + \bar{\nu}_\mu$ events) from the prolate Einasto profile with homogeneous annihilation cross-section enhancement. Middle: Atmospheric background (212446 $\nu_\mu + \bar{\nu}_\mu$ events) and DM annihilation contribution (1579 $\nu_\mu + \bar{\nu}_\mu$ events) from the prolate Einasto profile with $\propto r^{1/4}$ annihilation cross-section enhancement. As in Fig. 2 event numbers refer to the entire sky and we use the same mask of $|b| < 5^\circ$. Bottom left and bottom right: Same as the bottom plots of Fig. 2 for the cases of atmospheric background and XDM prolate Einasto without (left) and with (right) radial dependence. Due to its high sensitivity towards the GC and its good angular resolution KM3NeT would observe a clear signal from these models.

will be very clear even in the total counts. Known TeV γ -ray sources such as the H.E.S.S. J1745-290 [95–97] are also expected to contribute in that region. Yet the angular resolution of KM3NeT at ~ 1 TeV is expected to be below 1° [51]; thus given the already precise known location of these sources (from γ rays), it will be easy to account for their contribution, as has been done with γ -ray H.E.S.S. data [98] and with Fermi data [99].

With 10 years of data from KM3NeT the excess towards the GC will be very evident. About 8×10^3 DM events for the case of an Einasto prolate profile and 5×10^3 for the Einasto prolate profile with $\langle \sigma v \rangle \propto r^{1/4}$ will be detected.

In Fig. 4 we show the $\nu_\mu + \bar{\nu}_\mu$ reconstructed spectra from atmospheric and from XDM to muons after 3 years of observations in KM3NeT, from a window of $5^\circ < |b| < 15^\circ$ and $|l| < 5^\circ$, which was chosen to be optimal for a search of a signal from DM annihilation.

For an alternative comparison to Figs. 3 and 4, we also give in Table I the time scale in years for either IceCube or a telescope such as KM3NeT to observe 100 events from DM annihilation from the selected window of $5^\circ < |b| < 15^\circ$, $|l| < 5^\circ$ and an energy range of 1.0–1.3 TeV around which the neutrino spectrum of DM origin peaks. It is clear that a signal from XDM μ^\pm cannot be probed by IceCube in any reasonable time scale. Yet, a counterpart experiment in the Northern Hemisphere, with characteristics of those of the proposed KM3NeT, can detect such a signal within a few years.

The uncertainty in the atmospheric neutrino flux due to uncertainties in the pp collision production cross sections through the decay of π , K and σ mesons is expected to be up to $\sim 30\%$ at TeV energies [93]. Yet, this uncertainty cannot explain a change in the power law that would appear, *direction dependent*, in the galactic sky. For the case in Fig. 4 right ($\langle \sigma v \rangle \propto r^{1/4}$) the DM signal is too small to be detected. For the case of the Einasto prolate of Fig. 4 left, the break at ~ 2 TeV is not going to be very strong,

TABLE I. The time scale to observe 100 $\nu_\mu + \bar{\nu}_\mu$ upward events associated with signals of interest in IceCube (with an online filter) and in KM3NeT (assuming the HOURS simulation). In all the DM cases (XDM μ^\pm , $\chi\chi \rightarrow \mu^+\mu^-$ and $\chi\chi \rightarrow W^+W^-$), we use the same sky region of interest: $5^\circ < |b| < 15^\circ$, $|l| < 5^\circ$ (see main text for motivation) and an energy range of 1.0–1.3 TeV, around which these neutrino (observed) spectra peak. For the XDM μ^\pm case we show results for an Einasto prolate DM profile without (with) $r^{1/4}$ velocity induced suppression to the DM annihilation cross section. The same Einasto prolate profile for a homogeneous DM annihilation cross section is used for $\chi\chi \rightarrow \mu^+\mu^-$ and $\chi\chi \rightarrow W^+W^-$ with a spherical Einasto profile assumed in the results shown in the parentheses. For the Fermi bubbles we use the entire region of the bubbles and an energy range of 100 TeV to 1.0 PeV (100–130 TeV in parentheses).

Signal of interest	IceCube (yr)	KM3NeT (yr)
XDM μ^\pm 2.5 TeV	158 (294)	3.4 (5.8)
$\chi\chi \rightarrow \mu^+\mu^-$ 1.5 TeV	38 (168)	0.76 (3.3)
$\chi\chi \rightarrow W^+W^-$ 2.0 TeV	44 (193)	0.86 (3.8)
Fermi bubbles	9.0 (58)	0.11 (0.54)

even in that window. Yet, a gradual hardening of the total event spectra decreasing from high $|b|$ towards the galactic disk (excluding the $|b| < 5^\circ$ region) will be an indication of a signal from DM annihilation in the main DM halo. We expect that the power law of total reconstructed $\nu_\mu, \bar{\nu}_\mu$ events with energy between 300 GeV and 1.5 TeV *will become harder by 0.3* from the window of $|b| > 50^\circ$, $|l| < 5^\circ$ to that of $5^\circ < |b| < 15^\circ$, $|l| < 5^\circ$.

III. DARK MATTER ANNIHILATION TOWARDS THE GC, OTHER CHANNELS

Apart from the question of explaining the Fermi and WMAP haze signals via DM annihilation, the general connection of DM searches in neutrinos has received

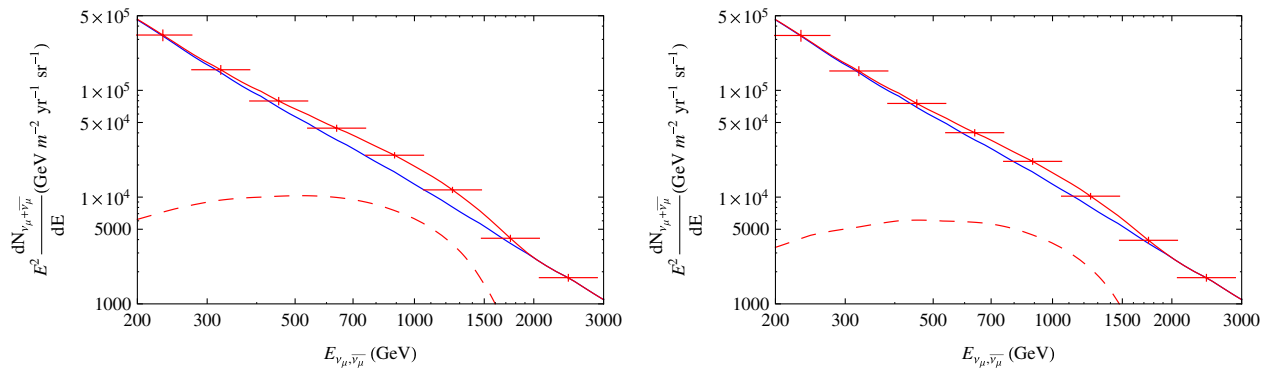


FIG. 4 (color online). KM3NeT $\nu_\mu + \bar{\nu}_\mu$ reconstructed spectra after 3 years within $5^\circ < |b| < 15^\circ$ and $|l| < 5^\circ$. Blue solid line: Atmospheric background flux. Red dashed line: DM only flux. Red solid line: atmospheric + DM flux. Left: Einasto prolate profile with homogeneous annihilation cross-section enhancement. Right: Einasto prolate profile with $\propto r^{1/4}$ with annihilation cross-section enhancement.

some attention in recent years, either from annihilation towards the GC [40,46,54] or from the DM annihilation captured in the Sun [41,45,100,101].

The Fermi and H.E.S.S. $e^- + e^+$ CR flux [19–21] and PAMELA positron [16] excesses, apart from the XDM models discussed in Sec. II, can be explained by a variety of other phenomenological channels [56,102–105].

For standard phenomenological models $\chi\chi \rightarrow W^+W^-$, $\chi\chi \rightarrow b\bar{b}$, strong limits have been placed using SUPER-K and IceCube observations towards the Sun (see, for example, some recent works of [41,100,101]).

Among the many models we choose to show results for the phenomenological models of DM annihilating directly to muons ($\chi\chi \rightarrow \mu^+\mu^-$) or directly to W bosons ($\chi\chi \rightarrow W^+W^-$), where electroweak corrections—especially important for the former channel—have been included [106,107]. These two channels are distinct from each other since for the one annihilating to muons high-energy neutrinos come from the decay of the boosted muons, while the $\chi\chi \rightarrow W^+W^-$ neutrinos are produced with a softer overall spectrum but at significantly higher multiplicity.

In Fig. 5 we show, for the window of $5^\circ < |b| < 15^\circ$, $|l| < 5^\circ$, the expected reconstructed upward fluxes in IceCube DeepCore of $\nu_\mu + \bar{\nu}_\mu$, for $\chi\chi \rightarrow \mu^+\mu^-$ with $m_\chi = 1.5$ TeV (left) and for $\chi\chi \rightarrow W^+W^-$ with $m_\chi = 2.0$ TeV (right).

The masses and annihilation cross sections are chosen to fit the Fermi, H.E.S.S. and PAMELA leptonic excesses given in [56]. We show results for two cases of DM profiles, the Einasto prolate profile of Eq. (1) (red lines) and the spherical Einasto profile (green lines). As can be seen for the more optimistic (to give a clear DM signal) prolate profile, a signal can be seen in IceCube DeepCore within 3 years of data for both channels. For the less

optimistic spherical Einasto profile, only in the case of $\chi\chi \rightarrow W^+W^-$ may a weak break at ≈ 2 TeV be seen.

Yet, in KM3NeT—which is near to optimal for searching for such a signal—after 3 years of data the reconstructed spectra in the same window will be measured with much greater statistics, as is shown in Fig. 6. Apart from the case of $\chi\chi \rightarrow \mu^+\mu^-$ with a spherical Einasto profile, all other cases give a clear break at the respective mass of the DM particle. For the case of $\chi\chi \rightarrow \mu^+\mu^-$ in the spherical Einasto, an indication of a signal will be the smooth hardening of the spectrum as one moves (using the same longitude range) from the high $|b|$ towards the disk, as discussed in Sec. II. In the specific case of $|b| > 40^\circ$ the power law is going to be ≈ 4.0 , while at $5^\circ < |b| < 15^\circ$ it is going to be ≈ 3.2 between energies of 300 GeV and 1.0 TeV. For a more cored profile the difference in the power law between the $|b| > 40^\circ$ region and the $5^\circ < |b| < 15^\circ$ region of the sky will be only 0.2.

An alternative indication of how much better a km^3 telescope in the Northern Hemisphere is compared to IceCube DeepCore for those types of searches is given in Fig. 7, where we show the reconstructed $\nu_\mu + \bar{\nu}_\mu$ within 500 GeV and 1.5 TeV for the $m_\chi = 1.5$ TeV, $\chi\chi \rightarrow \mu^+\mu^-$ case. For the IceCube DeepCore (left) and the KM3NeT (right) we use the reconstructed HOURS simulation [51]. For the entire DM halo (ignoring substructure) we show 368 $\nu_\mu + \bar{\nu}_\mu$ events (3 years) in IceCube DeepCore and 6482 for KM3NeT (3 years), with the equivalent background events being 2.2×10^4 and 1.4×10^5 . In Table I we also give, for both the $\chi\chi \rightarrow \mu^+\mu^-$ and the $\chi\chi \rightarrow W^+W^-$ channels, the time scale needed for each experiment to observe 100 $\nu_\mu + \bar{\nu}_\mu$ upward events from the direction of $5^\circ < |b| < 15^\circ$, $|l| < 5^\circ$ and in the energy range of 1.0–1.3 TeV (see also Figs. 5 and 6).

We note that current limits on the muon channel [the strongest of which come from dwarf spheroidal galaxies

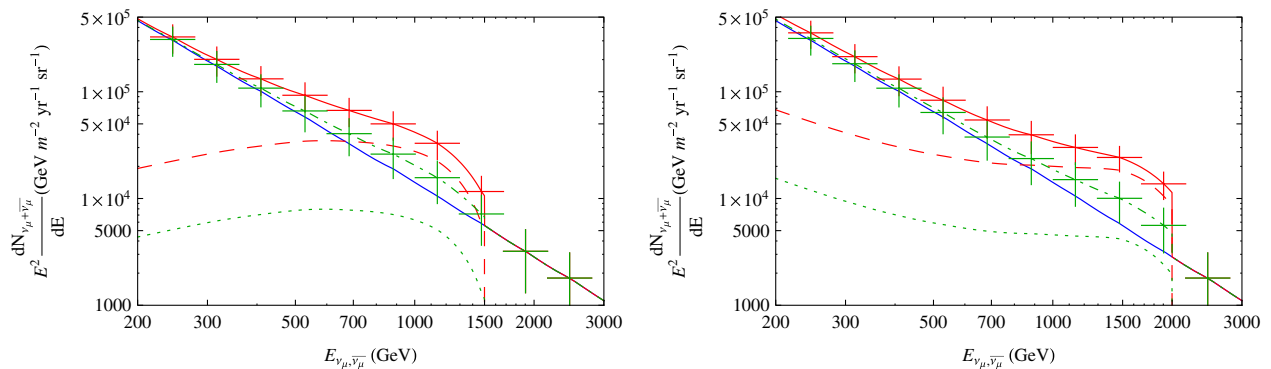


FIG. 5 (color online). IceCube DeepCore $\nu_\mu + \bar{\nu}_\mu$ reconstructed spectra after 3 years in the window of $5^\circ < |b| < 15^\circ$ and $|l| < 5^\circ$. Blue solid line: Atmospheric background flux. Red dashed and green dotted lines: DM only flux. Red solid and green dashed-dotted lines: Atmospheric + DM flux. Left: $\chi\chi \rightarrow \mu^+\mu^-$ Einasto prolate profile (red dashed/solid lines), and Einasto spherical profile (green dotted/dashed-dotted lines) with homogeneous annihilation cross-section enhancement. Right: $\chi\chi \rightarrow W^+W^-$ Einasto prolate (red dashed/solid lines), and Einasto spherical (green dotted/dashed-dotted lines) with homogeneous annihilation cross-section enhancement.

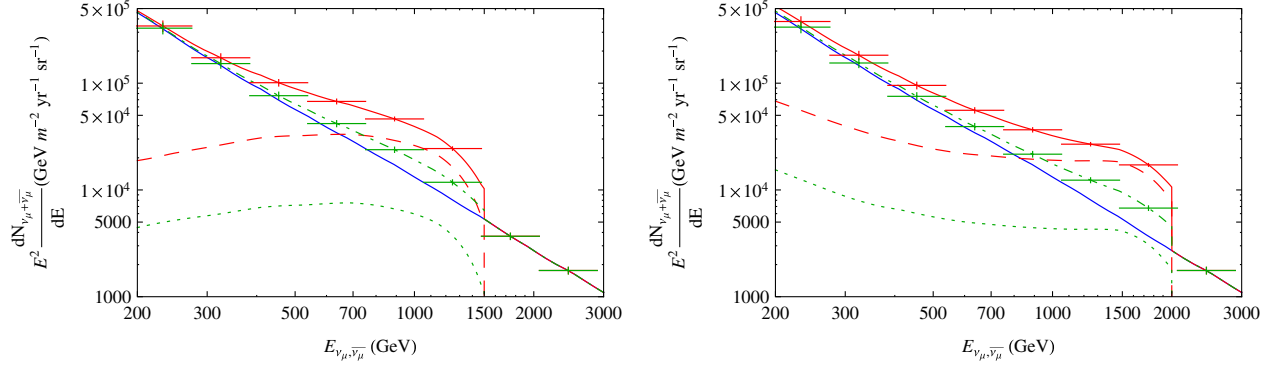


FIG. 6 (color online). KM3NeT $\nu_\mu + \bar{\nu}_\mu$ reconstructed spectra after 3 years in the window of $5^\circ < |b| < 15^\circ$ and $|l| < 5^\circ$. Blue solid line: Atmospheric background flux. Red dashed and green dotted lines: DM only flux. Red solid and green dashed-dotted lines: Atmospheric + DM flux. Left: $\chi\chi \rightarrow \mu^+\mu^-$ Einasto prolate profile (red dashed/solid lines), and Einasto spherical profile (green dotted/dashed-dotted lines) with homogeneous annihilation cross-section enhancement. Right: $\chi\chi \rightarrow W^+W^-$ Einasto prolate profile (red dashed/solid lines), and Einasto spherical (green dotted/dashed-dotted lines) with homogeneous annihilation cross-section enhancement.

(dSph) [108,109] cannot exclude a cross section of $\langle\sigma v\rangle \simeq 9.5 \times 10^{-24} \text{ cm}^3 \text{ s}^{-1}$ used here for the 1.5 TeV mass. For the case of $\chi\chi \rightarrow W^+W^-$ the cross section was taken to be $\simeq 7 \times 10^{-23} \text{ cm}^3 \text{ s}^{-1}$. This cross section is a factor of $\simeq 5$

times higher than conservative limits coming from dSph or antiprotons [36,37,110]. For the most optimistic cross sections that are still allowed by \bar{p} s and γ rays from dSphs, only for a very optimized DM halo profile

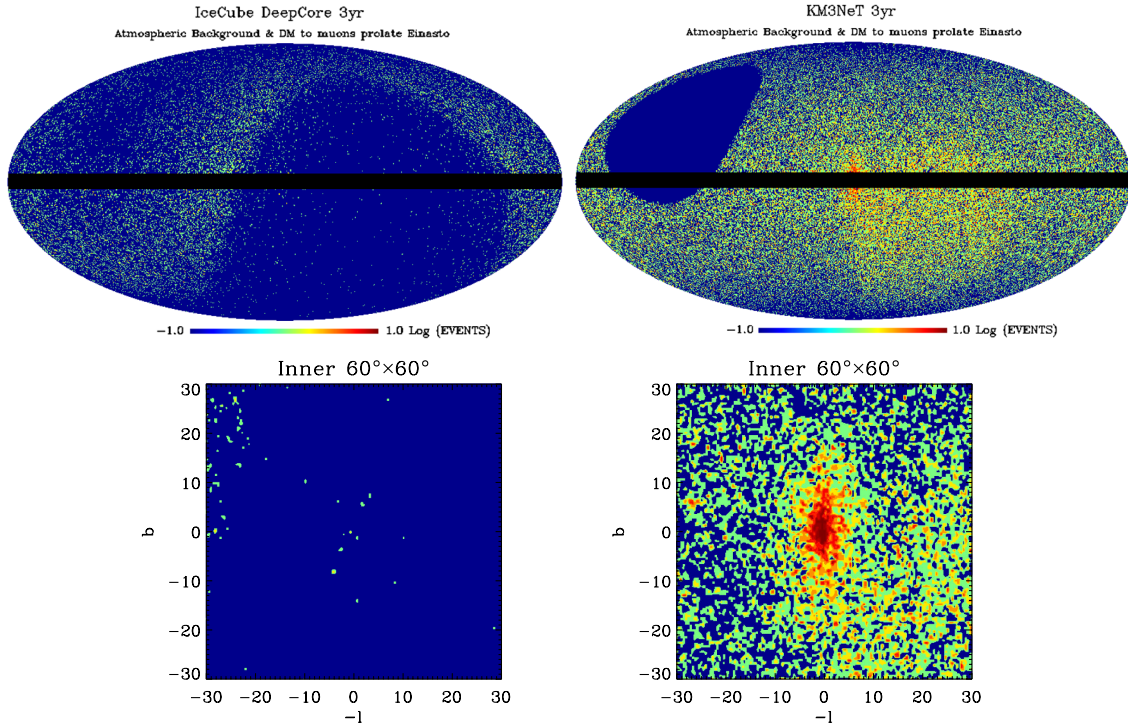


FIG. 7 (color online). $\nu_\mu + \bar{\nu}_\mu$ events with energy between 500 GeV and 1.5 TeV from DM annihilation of $M_\chi = 1.5 \text{ TeV}$ $\chi\chi \rightarrow \mu^+\mu^-$ Einasto prolate profile. Top left: With IceCube DeepCore in 3 years, with online filter atmospheric background (22477 $\nu_\mu + \bar{\nu}_\mu$ events) and contribution from DM (368 $\nu_\mu + \bar{\nu}_\mu$ events). Top right: With KM3NeT in 3 years using the HOURS reconstruction technique, atmospheric background (138560 $\nu_\mu + \bar{\nu}_\mu$ events) and contribution from DM (6482 $\nu_\mu + \bar{\nu}_\mu$ events). As in Fig. 2 event numbers refer to the entire sky and we use the same mask of $|b| < 5^\circ$. Bottom left and bottom right: Zooming in on the $60^\circ \times 60^\circ$ window for the IceCube (left) and KM3NeT (right) maps of the top row. Even in IceCube some excess of events is expected to be seen towards the GC. With KM3NeT sensitivity and angular resolution a clear signal from that model will be observed or strong constraints will be placed.

(such as a prolate or, in general, a cuspy profile) can there be a signal that would be detected. Thus, the neutrino searches for hadronic channels are deemed not optimal given how strong the constraints are that can be drawn from the local \bar{p} flux and from γ -ray searches for these channels. For leptonic to mainly muons channels though, \bar{p} s and γ rays provide weak constraints and neutrinos can provide a useful alternative search channel.

IV. HADRONIC SCENARIO: NEUTRINOS FROM THE FERMI BUBBLES

As discussed in [11] a possible explanation of the Fermi bubbles signal [2] is that of copious and long time-scale star formation in the galactic center giving CR protons with energies up to the PeV scale. These CR protons are transferred up to a distance of 10 kpc away from the galactic disk due to strong winds [11]. In that scenario the γ rays composing the Fermi bubbles will come from the decay chains of boosted mesons produced in pp collisions. The same process will produce neutrinos with energies up to the cutoff energy of these hard CR protons. Similarly these processes take place in the atmosphere producing the equivalent background.

The CR protons entering the atmosphere have a significantly softer spectrum (≈ 2.67 above 300 GeV) measured most recently from [111–113], compared to those responsible for the bubbles that have a spectrum described by [11]

$$\frac{dN_p}{dE_p} dE = N_0 E_p^{-2.1} \exp[-E_p/E_{p_0}], \quad (7)$$

with E_{p_0} the cutoff energy \sim PeV. Thus we can expect to see the neutrino component from the bubbles at high energies [13,15,116].

Another difference between the atmospheric neutrino background and the possible neutrino signal from the Fermi bubbles is that the CR protons entering the atmosphere due to column densities of matter \approx kg cm $^{-2}$ produce extensive showers that can reach, for the most energetic protons, up to 10^{10} particles at peak number [117–119], while for the CR protons at the bubbles region one expects much lower column densities [120]. Thus the possible Fermi bubbles' neutrinos cannot come from extensive showers, where products (protons mainly) from the hadronization of the initial pp collision would then hit on new target protons. Rather, the neutrinos will come from the decay chains of the hadronization products related to a single hard pp inelastic collision. This is an additional reason why the neutrinos from the bubbles have a harder spectrum than the atmospheric ones.

For the p-p inelastic processes the neutrinos are mainly produced from charged pion decays. For the neutrino spectra we follow the parametrization of [121], which was based on SIBYLL [122] simulations of pp collisions and is optimal at energies above 100 GeV that we care about.

The neutrinos coming from the bubbles will have the same morphology as the γ rays, which is relatively flat in longitude and latitude with clear edges [2]. However, it may not be trivial for the CR protons and the ISM target material transferred with them by the galactic winds to cause such a flat morphology in l and b , at γ rays; following the assumptions of [11] for the γ rays we will take the morphology of the neutrinos shown in Fig. 8 to be flat within the bubbles region, with clear edges as in the Fermi bubbles signal of [2].

As can be seen by comparing the morphology of Fig. 8 to that of Fig. 1, which are for neutrinos from DM scenarios that fit the Fermi and WMAP haze, the two types of morphologies are distinctively different. Moreover, the neutrino spectra and fluxes, as we will show, differ dramatically. In both Figs. 1 and 8 we show the same number of neutrino events without specifying the energy range or period of observation, and we are not taking into account that any actual neutrino telescope has (or will have) a strong angular dependence on its sensitivity. This is done to “spotlight” the different morphologies of the possible neutrino signals. Even after taking into account the specific properties of neutrino telescopes that we show results for, the different morphologies lead to searching for these signals in different parts of the sky.

The total energy stored in the CR protons in the bubbles is estimated to be $\sim 10^{56}$ erg due to an estimated averaged 10^{39} erg/s of injected power to hard CR protons transferred from the GC via galactic winds in the Fermi bubbles regions. This process is estimated to have been ongoing for a time scale of multiple Gyr [11]. These assumptions can result in a quasisteady state of injected energy from protons to γ , e^\pm and ν of $\dot{Q}_p \approx 3.6 \times 10^{38}$ erg/s from 10 GeV to 1 PeV [11]. Of that power from approximately equal partitions of energy to π^0 , π^+ and π^- , 1/3 goes to γ 's giving the better estimated power in the Fermi bubbles of $\approx 2 \times 10^{37}$ erg/s for γ rays with energy 1–100 GeV [2], or after extrapolation of the γ -ray spectrum, $\approx 1.2 \times 10^{38}$ erg/s for energies between 10 GeV and 1 TeV. Also,

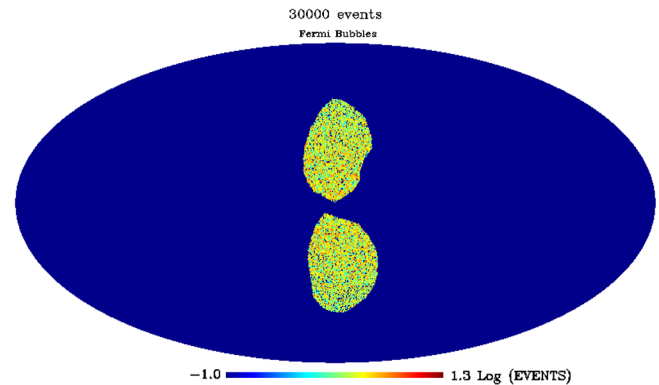


FIG. 8 (color online). Fermi bubbles, 3×10^4 simulated events.

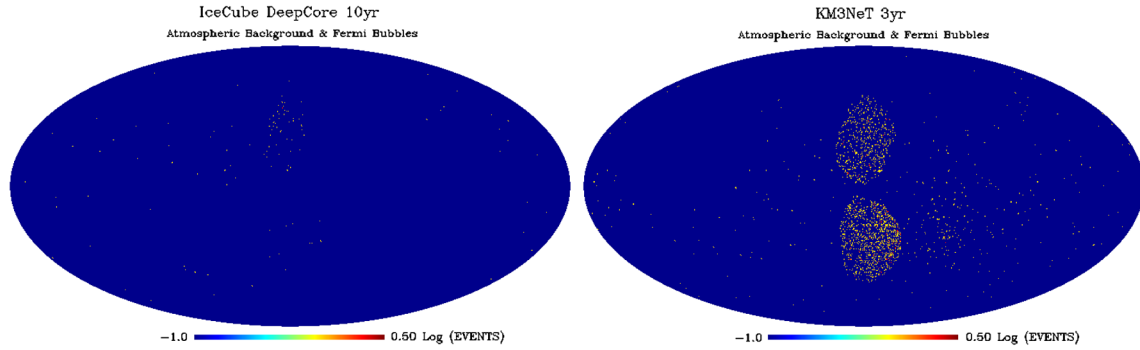


FIG. 9 (color online). $\nu_\mu + \bar{\nu}_\mu$ events, with energy between 100 TeV and 1.0 PeV. Right: With IceCube DeepCore in 10 years, with online filter atmospheric background (63 $\nu_\mu + \bar{\nu}_\mu$ events) and contribution from the Fermi bubbles (74 $\nu_\mu + \bar{\nu}_\mu$ events). Left: With KM3NeT in 3 years using HOURS reconstruction technique, atmospheric background (465 $\nu_\mu + \bar{\nu}_\mu$ events) and contribution from Fermi bubbles (1795 $\nu_\mu + \bar{\nu}_\mu$ events).

from the energy equipartition to the product pions we can estimate that the power to neutrinos is $\sim 2 \times 10^{38}$ erg/s inside the bubbles. We take the power to neutrinos to be 1×10^{38} erg/s, to account for an overestimation by a factor of 2 on the γ -ray luminosity of the bubbles by [11]. Assuming isotropic emission of ν 's inside the bubbles and a mean distance squared $D^2 \simeq R_{\text{sun}}^2 \simeq 8.5^2$ kpc² from us, we can estimate their flux. Their observed morphology as shown in Fig. 8 is isotropic within the bubbles.

In Fig. 9 (left) we show the expected $\nu_\mu + \bar{\nu}_\mu$ events mock map, with energy between 100 TeV and 1 PeV from IceCube DeepCore after 10 years of data collection. We show 74 events from the bubbles and 63 from the atmospheric background. In Fig. 9 (right) we also show what KM3NeT experiment with 3 years of reconstructed events would observe.

For the bubbles explanation of [11], choosing to mask out or not mask out the disk cannot affect the arguments on detecting the signal since most of the signal neutrino events are significantly above or below the disk.

Extragalactic point sources can also lead to an additional isotropic neutrino component at very high energies where the atmospheric background gets suppressed. Again, the same process (pp collisions) producing high-energy (\sim PeV) neutrinos will also produce γ rays with a spectrum that extends to lower energies. Due to the high sensitivity of the Fermi LAT instrument at the 0.1–100 GeV range, the more likely extragalactic sources to produce neutrinos have already been detected as point sources in γ rays as in [123]. With KM3NeT angular resolution of $>0.1^\circ$ above PeV energies, it will be very easy to associate even single neutrino events to known γ -ray point sources where pp collisions are expected to be the dominant mechanism for their production (as, for instance, in star-forming galaxies). Alternatively one can mask out known γ -ray point sources. Thus extragalactic point sources' contribution to the neutrino background can be accounted for. Finally, cosmogenic neutrinos from ultrahigh-energy CR (UHECR) protons interacting with

the cosmic microwave background (CMB) are already being constrained from the equivalent γ -ray spectrum at the Fermi LAT energies [124–127] and are expected to be a significant component only at energies above the $O(1)$ PeV range. Thus cosmogenic neutrinos do not contribute in the maps of Fig. 9, which show energies of neutrinos with $100 \text{ TeV} < E_{\nu_\mu, \bar{\nu}_\mu} < 1 \text{ PeV}$ [128].

The optimal region for IceCube DeepCore to search for a signal of bubbles at neutrinos would be the left part of the north bubble $10^\circ < b < 50^\circ$, $0^\circ < l < 20^\circ$, for which in Fig. 10 (left) we show the reconstructed fluxes from atmospheric and from bubbles after 3 years. Just based on that, one should soon expect a detection of the bubbles with IceCube DeepCore if the scenario of [11] is correct, or alternatively setting constraints on the hard CR proton component inside the bubbles.

With KM3NeT after 3 years, as we show in Fig. 9 (right), the optimal region is the part of the south bubble with $-50^\circ < b < -10^\circ$, $-20^\circ < l < 0^\circ$. A clear observation of the morphology (i.e. the south and right edges) would be expected. In Fig. 10 (right) we also show the reconstructed fluxes, which when/if observed at that level, would also provide a very good measurement of the injected energy to neutrinos (providing an alternative estimate of the CR protons' energy). Alternatively, lack of detection at KM3NeT should exclude the model of [11] as a possibility for the Fermi bubbles (see also Table I).

V. AGN AND ALTERNATE EXPLANATIONS FOR THE FERMI BUBBLES

An alternative explanation for the Fermi bubbles/haze to those of Secs. II and IV is strong AGN jet activity in the Galaxy as in [6,7]. The AGN case is supported by very recent evidence of γ -ray jets extending out from the galactic center, together with a 15° width and 40° – 45° length cocoon in the southern galactic hemisphere [129,130]. For the AGN scenario, the γ -ray signal is mainly from CR electrons with energies up to at least \sim TeV that up-scatter

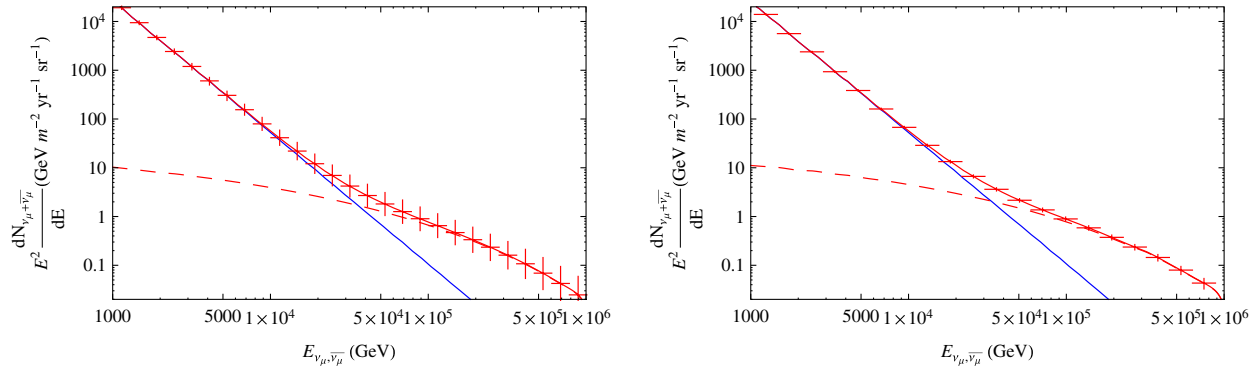


FIG. 10 (color online). $\nu_{\mu} + \bar{\nu}_{\mu}$ reconstructed spectra from Fermi bubbles. Blue solid line: Atmospheric background flux. Red dashed lines: Flux from bubbles. Red solid lines: Atmospheric + bubbles flux. Right: IceCube DeepCore with an online filter after 3 years of data in the window of $10^{\circ} < b < 50^{\circ}$ and $0^{\circ} < l < 20^{\circ}$. Left: KM3NeT with HOURS reconstruction after 3 years of data in the window of $-50^{\circ} < b < -10^{\circ}$ and $-20^{\circ} < l < 0^{\circ}$.

the local radiation field (mainly CMB at high latitudes). CR protons cannot contribute much of the observed γ -ray signal since the ISM gas targets have a very low density at high distances (up to 10 kpc) above the disk. Given the CR energy density profiles from the MHD simulations of [6], it will be very difficult for CR protons to explain the morphology of the bubbles that are relatively flat in latitude, suggesting a limb brightening [9]. Thus the scenario of [6] may give only a few neutrino events at high latitudes.

In the first [10] and second [9] order Fermi acceleration scenarios, some protons would also be accelerated at high energies with power-law spectral indices (for the differential spectrum) of E^{-2} and E^{-1} [9], respectively. Since those protons would not lose their energy fast (compared to the CR electrons), the CR proton spectra would be homogeneous within the bubbles. Yet, in both scenarios the explanation of the γ -ray signal is entirely from the leptonic components. The protons (at least in those basic scenarios) are not expected to contribute much to the γ -ray signal, especially since in order for protons to contribute significantly to the bubbles signal, much greater amounts of total energy to accelerated CRs are needed than in the models of [9,10,131]. As an example, in the mechanism presented in [9], the needed total energy in CR electrons above 100 MeV is $\sim 10^{51}$ erg, while for the hadronic model of [11] the total energy in CR protons is $\sim 10^{56}$ erg. Thus we do not expect a significant number of neutrinos from the leptonic models of [9,10] either.

VI. CONCLUSIONS

The recent uncovering of the Fermi bubbles/haze [1,2] in the Fermi γ -ray data has generated theoretical work in explaining such a signal in combination (or not) with the WMAP haze signal of [4,5].

We have shown that for the DM explanation of the combined Fermi haze and WMAP haze as in [3] under the annihilation channel to muons that is optimal for neutrinos (XDM [55] annihilation to μ^{\pm}) and for a prolate

DM halo, we can observe a counterpart signal with a km^3 telescope located in the Northern Hemisphere at ~ 3 years of data collection (see discussion in Sec. II and Figs. 3 and 4). IceCube DeepCore and ANTARES will not observe any signal for such a model, while for the case of XDM annihilation to e^{\pm} through a very light scalar boson $\phi < 2m_{\mu}$, no neutrinos are produced.

For other channels/models of DM annihilation that produce more neutrinos either from larger suggested boost factors as in $\chi\chi \rightarrow \mu^+\mu^-$ for the explanation of the Fermi $e^+ + e^-$ signal (see, for example, [39]), or due to large hadronic branching ratios as in $\chi\chi \rightarrow W^+W^-$, the neutrino events are enhanced significantly. Some signal from DM is expected even after excluding the disk region where nonatmospheric backgrounds are concentrated (see Fig. 7). Yet neutrinos cannot provide the strongest limits for the hadronic channels of annihilating DM. For the leptonic annihilation to muons case, the limits can be useful though, since they can be more robust than the pretty weak limits from γ 's and \bar{p} [35–38,109,110].

For the Fermi bubbles explanation of [11], a significant number of >10 TeV neutrinos is estimated, and even with IceCube DeepCore we should expect detection or limits (see Figs. 9 and 10). Furthermore, a km^3 telescope in the Northern Hemisphere will either exclude the model of [11] or confirm the morphology of the bubbles at neutrinos and measure the power injected to neutrinos from inelastic pp collisions inside the bubbles as we show in Figs. 9 and 10.

Leptonic scenarios for the Fermi bubbles such as those of [6,9,10] would also predict some CR protons, but are not expected to give any significant neutrino signal, since the main source for the γ rays is IC scattering from CR electrons.

With the current IceCube DeepCore telescope a first probe of some of the models of the Fermi bubbles/haze can be achieved, while with a km^3 telescope located in the Northern Hemisphere, discrimination between the hadronic [11], the leptonic [6,9,10] and the DM [3] cases will be attained.

As this paper was being written, a new analysis of Fermi γ rays suggested the evidence of γ -ray jets in the Milky Way extending out to ~ 10 kpc from the galactic center [129]. Additionally, a cocoon structure has been revealed in the southern galactic hemisphere. While according to [129] the total luminosity of the north and the south jetlike features is $(1.8 \pm 0.35) \times 10^{35}$ erg/s at 1–100 GeV, i.e. 2 orders of magnitude less in luminosity than the bubbles (2×10^{37} erg/s in the same energy range), such an additional signal favors the AGN case, with the bubbles coming from the decelerated jet material [129].

Yet the two signals, i.e. the combined γ -ray cocoon and jets and the Fermi bubbles, may be created at a different time. Such a case would allow for a combination of sources, DM and AGN, hadronic model and AGN, to account for the total γ -ray bubbles/haze and jets and cocoon signals. For the hybrid scenario of DM and AGN, the edge at $l > 0$ (left) of the south bubble could just be the result of the presence (overlap on the sky) of the AGN cocoon, and thus morphologically would not need to be explained by DM annihilation. Similarly, a cocoon in the

northern galactic hemisphere (not claimed to be clearly revealed yet) could account for the edge north to the right (at $l < 0$) in the data. Additionally the AGN responsible for the jets and the cocoon of [129] could evacuate the cavity of the bubbles which the high-energy e^\pm from annihilating DM then fill [3].

Since the luminosity of the jets alone is only 1% of that of the bubbles/haze, assuming that the current state of the jets is representative of the time-averaged state [132], the predictions for the neutrino fluxes from the DM/hadronic cases remain the same [133].

ACKNOWLEDGMENTS

The author would like to thank Gregory Dobler, Douglas Finkbeiner, Maryam Tavakoli, Aikaterini Tzamarioudaki, Spyros Tzamaras, Piero Ullio and Neal Weiner for valuable discussions. The author would also like to specifically thank Apostolos Tsirigotis for offering information regarding the HOURS simulation of events reconstruction in KM3NeT.

-
- [1] G. Dobler, D. P. Finkbeiner, I. Cholis, T. R. Slatyer, and N. Weiner, *Astrophys. J.* **717**, 825 (2010).
 - [2] M. Su, T. R. Slatyer, and D. P. Finkbeiner, *Astrophys. J.* **724**, 1044 (2010).
 - [3] G. Dobler, I. Cholis, and N. Weiner, *Astrophys. J.* **741**, 25 (2011).
 - [4] D. P. Finkbeiner, *Astrophys. J.* **614**, 186 (2004).
 - [5] G. Dobler and D. P. Finkbeiner, *Astrophys. J.* **680**, 1222 (2008).
 - [6] F. Guo and W. G. Mathews, *Astrophys. J.* **756**, 181 (2012).
 - [7] F. Guo, W. G. Mathews, G. Dobler, and S. Oh, *Astrophys. J.* **756**, 182 (2012).
 - [8] I. Cholis and N. Weiner, [arXiv:0911.4954](https://arxiv.org/abs/0911.4954).
 - [9] P. Mertsch and S. Sarkar, *Phys. Rev. Lett.* **107**, 091101 (2011).
 - [10] K. Cheng, D. Chernyshov, V. Dogiel, C.-M. Ko, and W.-H. Ip, *Astrophys. J.* **731**, L17 (2011).
 - [11] R. M. Crocker and F. Aharonian, *Phys. Rev. Lett.* **106**, 101102 (2011).
 - [12] D. Malyshev, I. Cholis, and J. D. Gelfand, *Astrophys. J.* **722**, 1939 (2010).
 - [13] F. Vissani and F. Aharonian, *Nucl. Instrum. Methods Phys. Res., Sect. A* **692**, 5 (2012).
 - [14] T. K. Gaisser and T. Stanev, *Astropart. Phys.* **39-40**, 120 (2012).
 - [15] C. Lunardini and S. Razzaque, *Phys. Rev. Lett.* **108**, 221102 (2012).
 - [16] M. Boezio *et al.*, [arXiv:0810.3508](https://arxiv.org/abs/0810.3508).
 - [17] O. Adriani *et al.* (PAMELA), *Nature (London)* **458**, 607 (2009).
 - [18] O. Adriani *et al.*, *Phys. Rev. Lett.* **102**, 051101 (2009).
 - [19] F. Aharonian *et al.* (H.E.S.S.), *Phys. Rev. Lett.* **101**, 261104 (2008).
 - [20] F. Aharonian *et al.* (H.E.S.S.), *Astron. Astrophys.* **508**, 561 (2009).
 - [21] A. A. Abdo *et al.* (Fermi LAT), *Phys. Rev. Lett.* **102**, 181101 (2009).
 - [22] J. Chang *et al.*, *Nature (London)* **456**, 362 (2008).
 - [23] N. Arkani-Hamed, D. P. Finkbeiner, T. R. Slatyer, and N. Weiner, *Phys. Rev. D* **79**, 015014 (2009).
 - [24] I. Cholis, D. P. Finkbeiner, L. Goodenough, and N. Weiner, *J. Cosmol. Astropart. Phys.* **12** (2009) 007.
 - [25] R. Harnik and G. D. Kribs, *Phys. Rev. D* **79**, 095007 (2009).
 - [26] P. J. Fox and E. Poppitz, *Phys. Rev. D* **79**, 083528 (2009).
 - [27] P. Grajek, G. Kane, D. Phalen, A. Pierce, and S. Watson, *Phys. Rev. D* **79**, 043506 (2009).
 - [28] M. Pospelov and A. Ritz, *Phys. Lett. B* **671**, 391 (2009).
 - [29] J. D. March-Russell and S. M. West, *Phys. Lett. B* **676**, 133 (2009).
 - [30] M. Cirelli and A. Strumia, *New J. Phys.* **11**, 105005 (2009).
 - [31] W. Shepherd, T. M. Tait, and G. Zaharijas, *Phys. Rev. D* **79**, 055022 (2009).
 - [32] D. J. Phalen, A. Pierce, and N. Weiner, *Phys. Rev. D* **80**, 063513 (2009).
 - [33] D. Hooper and K. M. Zurek, *Phys. Rev. D* **79**, 103529 (2009).
 - [34] D. Hooper and T. M. Tait, *Phys. Rev. D* **80**, 055028 (2009).
 - [35] M. Cirelli, M. Kadastik, M. Raidal, and A. Strumia, *Nucl. Phys.* **B813**, 1 (2009).
 - [36] F. Donato, D. Maurin, P. Brun, T. Delahaye, and P. Salati, *Phys. Rev. Lett.* **102**, 071301 (2009).

- [37] I. Cholis, *J. Cosmol. Astropart. Phys.* **09** (2011) 007.
- [38] C. Evoli, I. Cholis, D. Grasso, L. Maccione, and P. Ullio, *Phys. Rev. D* **85**, 123511 (2012).
- [39] L. Bergstrom, J. Edsjo, and G. Zaharijas, *Phys. Rev. Lett.* **103**, 031103 (2009).
- [40] A.E. Erkoca, G. Gelmini, M.H. Reno, and I. Sarcevic, *Phys. Rev. D* **81**, 096007 (2010).
- [41] S.K. Mandal, M.R. Buckley, K. Freese, D. Spolyar, and H. Murayama, *Phys. Rev. D* **81**, 043508 (2010).
- [42] I.F. Albuquerque, L.J. Beraldo e Silva, and C. Perez de los Heros, *Phys. Rev. D* **85**, 123539 (2012).
- [43] R. Abbasi *et al.* (IceCube Collaboration), *Astrophys. J.* **732**, 18 (2011).
- [44] S. Sarkar (IceCube Collaboration), *Astropart. Phys.* **35**, 615 (2012).
- [45] R. Abbasi *et al.* (IceCube Collaboration), [arXiv:1111.2738](https://arxiv.org/abs/1111.2738).
- [46] C.d.l. Heros, Proc. Sci., IDM2010 (2011) 064 [[arXiv:1012.0184](https://arxiv.org/abs/1012.0184)].
- [47] R. Abbasi *et al.* (IceCube Collaboration), *Phys. Rev. D* **84**, 022004 (2011).
- [48] S. Adrian-Martinez *et al.* (Antares Collaboration), *Astrophys. J.* **743**, L14 (2011).
- [49] C. Bogazzi (ANTARES Collaboration), [arXiv:1112.0478](https://arxiv.org/abs/1112.0478).
- [50] A. Heijboer (ANTARES Collaboration), *Nucl. Instrum. Methods Phys. Res., Sect. A* **662**, S216 (2012).
- [51] A. Tsigotis, A. Leisos, S. Tzamarias (o. b. o. t. K. Consortium), [arXiv:1201.5079](https://arxiv.org/abs/1201.5079) [*Nucl. Instrum. Methods Phys. Res., Sect. A* (to be published)].
- [52] A. Leisos, A. Tsigotis, and S. Tzamarias (KM3NeT Consortium), [arXiv:1201.5584](https://arxiv.org/abs/1201.5584) [*Nucl. Instrum. Methods Phys. Res., Sect. A* (to be published)].
- [53] <http://www.km3net.org/home.php>, <http://www.km3net.org/public.php>.
- [54] A.E. Erkoca, M.H. Reno, and I. Sarcevic, *Phys. Rev. D* **82**, 113006 (2010).
- [55] D.P. Finkbeiner and N. Weiner, *Phys. Rev. D* **76**, 083519 (2007).
- [56] I. Cholis, G. Dobler, D.P. Finkbeiner, L. Goodenough, and N. Weiner, *Phys. Rev. D* **80**, 123518 (2009).
- [57] D.P. Finkbeiner, L. Goodenough, T.R. Slatyer, M. Vogelsberger, and N. Weiner, *J. Cosmol. Astropart. Phys.* **05** (2011) 002.
- [58] J. Diemand, M. Kuhlen, P. Madau, M. Zemp, B. Moore, D. Potter, and J. Stadel, *Nature (London)* **454**, 735 (2008).
- [59] M. Kuhlen, J. Diemand, P. Madau, and M. Zemp, *J. Phys. Conf. Ser.* **125**, 012008 (2008).
- [60] V. Springel, J. Wang, M. Vogelsberger, A. Ludlow, A. Jenkins, A. Helmi, J.F. Navarro, C.S. Frenk, and S.D.M. White, *Mon. Not. R. Astron. Soc.* **391**, 1685 (2008).
- [61] A.R. Zentner, A.V. Kravtsov, O.Y. Gnedin, and A.A. Klypin, *Astrophys. J.* **629**, 219 (2005).
- [62] J. Bailin, D. Kawata, B.K. Gibson, M. Steinmetz, J.F. Navarro *et al.*, *Astrophys. J.* **627**, L17 (2005).
- [63] The BR to muons for $2m_\mu < m_\phi < 2m_\pi$ can be dominant for a scalar ϕ .
- [64] A. Sommerfeld, *Ann. Phys. (Berlin)* **403**, 257 (1931).
- [65] M. Lattanzi and J.I. Silk, *Phys. Rev. D* **79**, 083523 (2009).
- [66] J. Hisano, S. Matsumoto, M. Nagai, O. Saito, and M. Senami, *Phys. Lett. B* **646**, 34 (2007).
- [67] B. Robertson and A. Zentner, *Phys. Rev. D* **79**, 083525 (2009).
- [68] T.R. Slatyer, N. Toro, and N. Weiner, *Phys. Rev. D* **86**, 083534 (2012).
- [69] R. Catena and P. Ullio, *J. Cosmol. Astropart. Phys.* **08** (2010) 004.
- [70] P. Salucci, F. Nesti, G. Gentile, and C. Martins, *Astron. Astrophys.* **523**, A83 (2010).
- [71] D. Merritt, J.F. Navarro, A. Ludlow, and A. Jenkins, *Astrophys. J.* **624**, L85 (2005).
- [72] E. Romano-Diaz, I. Shlosman, C. Heller, and Y. Hoffman, *Astrophys. J.* **702**, 1250 (2009).
- [73] S.E. Pedrosa, P.B. Tissera, and C. Scannapieco, [arXiv:0910.4380](https://arxiv.org/abs/0910.4380) [*Mon. Not. R. Astron. Soc.* (to be published)].
- [74] P.B. Tissera, S.D. White, S. Pedrosa, and C. Scannapieco, [arXiv:0911.2316](https://arxiv.org/abs/0911.2316) [*Mon. Not. R. Astron. Soc.* (to be published)].
- [75] O.H. Parry, V.R. Eke, C.S. Frenk, and T. Okamoto, [arXiv:1105.3474](https://arxiv.org/abs/1105.3474).
- [76] J. Binney and S. Tremaine, *Galactic Dynamics: Second Edition* (Princeton University Press, Princeton, NJ, 2008).
- [77] For IceCube and KM3NeT the expected angular resolution of the reconstructed events is expected to be a few degrees [43,51,78].
- [78] D. Lenis and G. Stavropoulos, [arXiv:1203.6727](https://arxiv.org/abs/1203.6727).
- [79] P.M.W. Kalberla and L. Dedes, *Astron. Astrophys.* **487**, 951 (2008).
- [80] P.M.W. Kalberla, L. Dedes, J. Kerp, and U. Haud, *Astron. Astrophys.* **469**, 511 (2007).
- [81] L. Bronfman, R.S. Cohen, H. Alvarez, J. May, and P. Thaddeus, *Astrophys. J.* **324**, 248 (1988).
- [82] H. Nakanishi and Y. Sofue, *Publ. Astron. Soc. Jpn.* **58**, 847 (2006).
- [83] For profiles in diffuse γ rays of the equivalent “ π^0 ” component see [84].
- [84] Fermi-LAT Collaboration, *Astrophys. J.* **750**, 3 (2012).
- [85] C. Evoli, D. Grasso, and L. Maccione, *J. Cosmol. Astropart. Phys.* **06** (2007) 003.
- [86] For a Majorana particle.
- [87] T.E. Tsigotis A.G. Tzamarias, and A. Tzamarioudaki (private communication).
- [88] G. Barenboim and C. Quigg, *Phys. Rev. D* **67**, 073024 (2003).
- [89] K. Murase, *Phys. Rev. D* **76**, 123001 (2007).
- [90] The charged current and neutral current neutrino nucleon cross sections are different for ν_μ and $\bar{\nu}_\mu$ [40,91]. Here we use averaged values of A_{ν_μ} , $A_{\bar{\nu}_\mu}$. For the DM annihilation cases that we study the ν_μ and $\bar{\nu}_\mu$ fluxes arriving at Earth are equal.
- [91] A. Strumia and F. Vissani, [arXiv:hep-ph/0606054](https://arxiv.org/abs/hep-ph/0606054).
- [92] I. Cholis, L. Goodenough, and N. Weiner, *Phys. Rev. D* **79**, 123505 (2009).
- [93] M. Honda, T. Kajita, K. Kasahara, S. Midorikawa, and T. Sanuki, *Phys. Rev. D* **75**, 043006 (2007).
- [94] Similar results for DM and atmospheric neutrinos in KM3NeT come from simulations like those of [78].
- [95] F. Aharonian *et al.* (HESS Collaboration), *Astron. Astrophys.* **425**, L13 (2004).

- [96] C. van Eldik *et al.* (HESS Collaboration), *J. Phys. Conf. Ser.* **110**, 062003 (2008).
- [97] F. Aharonian (H.E.S.S. Collaboration), *Astron. Astrophys.* **503**, 817 (2009).
- [98] F. Aharonian *et al.* (H.E.S.S. Collaboration), *Phys. Rev. Lett.* **97**, 221102 (2006).
- [99] D. Hooper and L. Goodenough, *Phys. Lett. B* **697**, 412 (2011).
- [100] C. A. Argüelles and J. Kopp, *J. Cosmol. Astropart. Phys.* **07** (2012) 016.
- [101] V. Barger, J. Kumar, D. Marfatia, and E. M. Sessolo, *Phys. Rev. D* **81**, 115010 (2010).
- [102] M. Cirelli and A. Strumia, *Proc. Sci.*, IDM2008 (2008) 089 [arXiv:0808.3867].
- [103] L. Bergstrom, T. Bringmann, and J. Edsjo, *Phys. Rev. D* **78**, 103520 (2008).
- [104] I. Cholis, L. Goodenough, D. Hooper, M. Simet, and N. Weiner, *Phys. Rev. D* **80**, 123511 (2009).
- [105] J. Zhang, X-J. Bi, J. Liu, S-M. Liu, P-F. Yin, Q. Yuan, and S-H. Zhu, *Phys. Rev. D* **80**, 023007 (2009).
- [106] P. Ciafaloni, D. Comelli, A. Riotto, F. Sala, A. Strumia, and A. Urbano, *J. Cosmol. Astropart. Phys.* **03** (2011) 019.
- [107] M. Cirelli, G. Corcella, A. Hektor, G. Hutsi, M. Kadastik, P. Panci, M. Raidal, F. Sala, and A. Strumia, *J. Cosmol. Astropart. Phys.* **03** (2011) 051. All results are available at <http://www.marcocirelli.net/PPPC4DMID.html>.
- [108] M. Ackermann *et al.* (Fermi-LAT Collaboration), *Phys. Rev. Lett.* **107**, 241302 (2011).
- [109] I. Cholis and P. Salucci, *Phys. Rev. D* **86**, 023528 (2012).
- [110] M. Cirelli, R. Franceschini, and A. Strumia, *Nucl. Phys. B* **800**, 204 (2008).
- [111] O. Adriani *et al.* (PAMELA Collaboration), *Science* **332**, 69 (2011).
- [112] Y. S. Yoon *et al.*, *Astrophys. J.* **728**, 122 (2011).
- [113] Older measurements suggest a value for the power law of the differential spectrum closer to 2.7–2.8 at the multi-TeV scale [114,115] and thus slightly softer spectra.
- [114] K. Asakimori, T.H. Burnett, M.L. Cherry, K. Chebli, M.J. Christ, S. Dake, J.H. Derrickson, W.F. Fountain, M. Fuki, J.C. Gregory *et al.*, *Astrophys. J.* **502**, 278 (1998).
- [115] V. A. Derbina, V.I. Galkin, M. Hareyama, Y. Hiraoka, Y. Horiuchi, M. Ichimura, N. Inoue, E. Kamioka, T. Kobayashi, V.V. Kopenkin *et al.*, *Astrophys. J. Lett.* **628**, L41 (2005).
- [116] R.M. Crocker, D.I. Jones, F. Aharonian, C.J. Law, F. Melia, T. Oka, and J. Ott, *Mon. Not. R. Astron. Soc.* **413**, 763 (2011).
- [117] J. Abraham *et al.* (Pierre Auger Collaboration), *Astropart. Phys.* **32**, 89 (2009).
- [118] J. Matthews, *Astropart. Phys.* **22**, 387 (2005).
- [119] M. S. Longair, *High Energy Astrophysics* (Cambridge University Press, Cambridge, England, 2002), Vol. 1, pp. 286–291.
- [120] As a comparison to the GC the ISM column density is $\approx 10^{-4}$ kg cm $^{-2}$.
- [121] S.R. Kelner, F.A. Aharonian, and V.V. Bugayov, *Phys. Rev. D* **74**, 034018 (2006).
- [122] R. Fletcher, T. Gaisser, P. Lipari, and T. Stanev, *Phys. Rev. D* **50**, 5710 (1994).
- [123] P.L. Nolan *et al.* (T.F.-L. Collaboration), *Astrophys. J. Suppl. Ser.* **199**, 31 (2012).
- [124] V. Berezhinsky, A. Gazizov, M. Kachelriess, and S. Ostapchenko, *Phys. Lett. B* **695**, 13 (2011).
- [125] M. Ahlers, L. Anchordoqui, M. Gonzalez-Garcia, F. Halzen, and S. Sarkar, *Astropart. Phys.* **34**, 106 (2010).
- [126] G. Decerprit and D. Allard, *Astron. Astrophys.* **535**, A66 (2011).
- [127] K. Murase, J.F. Beacom, and H. Takami, *J. Cosmol. Astropart. Phys.* **08** (2012) 030.
- [128] For IceCube DeepCore an $O(1)$ neutrino event per year is estimated for proton composition of UHECRs [125].
- [129] M. Su and D.P. Finkbeiner, *Astrophys. J.* **753**, 61 (2012).
- [130] D.P. Finkbeiner. (private communication).
- [131] Also since for CR protons to give γ rays pp collisions are necessary, the morphology of the γ -ray signal from these accelerated protons is not expected to be similar to that of the ICS γ rays from the accelerated electrons.
- [132] As noted by D. Finkbeiner if currently the jets are at a low luminosity phase, then the time-averaged luminosity of the jets could be much higher [130]. In such a case the entire bubbles signal could come from AGN activity.
- [133] The spectrum of the cocoon revealed only in the southern galactic hemisphere is similar to that of the jets and the bubbles [129] but still covers only part of the south bubble angular region; thus it cannot account for the major part of the south bubble γ -ray luminosity.
- [134] K. Gorski, E. Hivon, A. Banday, B. Wandelt, F. Hansen, M. Reinecke, and M. Bartelmann, *Astrophys. J.* **622**, 759 (2005).